Nonlinear Dynamics and Systems Theory, **4**(1) (2004) 73–88

Effects of Substantial Mass Loss on the Attitude Motions of a Rocket-Type Variable Mass System

J. Sookgaew and F.O. Eke

Department of Mechanical and Aeronautical Engineering, University of California at Davis, One Shields Avenue Davis, CA 95616 USA

Received: September 10, 2003; Revised: March 12, 2004

Abstract: This study uses a relatively complex model to analyze the influence of various system parameters on the attitude behavior of a rocket-type variable mass system moving in a torque-free environment. Some of the parameters studied include the system's size, the nozzle expansion ratio, and the location of the propellant within the system's casing. Results obtained indicate that the spin rate as well as the transverse rate can increase, decrease, or stay constant depending on the choice of system parameters. Dramatic changes in the character of these variables can result from relatively minor changes in a rocket's nozzle expansion ratio.

Keywords: *Variable mass processes; rockets.*

Mathematics Subject Classification (2000): 70P05, 70M20, 34C60.

1 Introduction

The behavior of mechanical systems with varying mass is of interest to scientists and engineers because of the vast array of physical systems (both natural and engineered) that exhibit variable mass characteristics. Aerospace systems have high visibility as variable mass systems, and are the main focus of this study.

One of the earliest studies of the dynamics of variable mass systems was performed by Buquoy [1]. He developed his "motion formula" for these systems, and presented solutions to a large number of examples in this area. Another early and major contributor to the field is Meshcherskii [8, 9], who essentially laid the foundation for the theoretical study of variable mass systems in mechanics. The focus of practically all the early work in this area was on the translational motion of such systems. This paper investigates the rotational dynamics of rocket-type variable mass systems in a torque-free environment.

Attitude dynamics studies of rotating bodies usually involve the derivation of the equations of motion of the system of interest, followed by some attempt at extracting useful motion information from these equations. Strategies for the development of equations of motion of mechanical systems, especially those with a solid base, have been presented by a number of authors (see, for example, Kovalev [5], Eke and Wang [3]). For variable mass systems in general, and rocket systems in particular, equation derivation can proceed along one of at least two different paths — the discrete model approach, and the control volume method. When used in the study of rocket-type systems, the discrete model approach introduces simplifying assumptions very early in the equation derivation process. For example, it is common in this approach to consider that all the particles leaving the system during a propellant burn, do so at the same velocity relative to the main rocket body, and that this relative velocity is always parallel to the rocket axis. This method was popularized by Thomson in the 1960's [11 – 13], and was effectively used by him and others in the analysis of rocket motion.

The control volume approach starts by viewing the system, in a general way, as consisting of solid and fluid phases contained in a region that is delimited by a closed surface of constant or variable internal volume. Equations of motion for such a general variable mass system are then derived using well-known methods of fluid and classical dynamics. At this stage, the resulting equations are generally very complex, containing several surface and volume integrals. They are then reduced to tractable forms by specializing them to the specific system under study. Thus, unlike the discrete model approach, the control volume method introduces most of its simplifying assumptions at the end of the equation derivation process. Equations of motion derived in this way are now readily available in the literature (see, for example, references [2, 3, 7]).

There are three basic types of physical model that have been used in the study of the dynamics of rocket systems: the variable mass cylinder, the general axisymmetric model, and the two-body axisymmetric system. The variable mass cylinder models a typical rocket system as a simple right circular cylinder. Wang, Eke, and Mao [4, 6] exploited such a simple-minded model to great advantage. Its main merit is its simplicity; yet, surprisingly, it does capture a great deal of the important features of a real rocket. The disadvantage is that it does not permit certain refinements in the study. For example, the model does not include a nozzle, and so, nozzle effects cannot be explored. Nor is it possible to study the effect of the geometric location of the propellant grain within a rocket system, since the model normally views the whole of the cylinder as combustible.

The general axisymmetric model represents a rocket as an axisymmetric body (not just a cylinder) of diminishing mass and inertia [7]. In this case, the manner in which the system's inertia properties vary with mass depletion is not known and cannot be precisely determined. Because of this shortcoming, it is difficult to push analytical studies of the system's motion to their limit; one is thus limited to qualitative inferences in this case. Some authors have tried to circumvent this difficulty by assigning simple, decreasing functions of time to the mass, as well as to the axial and the transverse inertia. The difficulty with such a strategy is that the transverse and axial inertia scalars vary in a dependent manner as the system's mass decreases. It is thus next to impossible to make correct guesses for all the inertia functions as well as the system mass. This problem is discussed in some detail in reference [6].

The two-body axisymmetric model is the most versatile of the three models mentioned above. It separates the system into two parts — a constant mass part, and a variable mass portion. In a rocket system for example, the fuel or propellant would represent the variable mass part, and the other parts of the system outside the fuel would be the

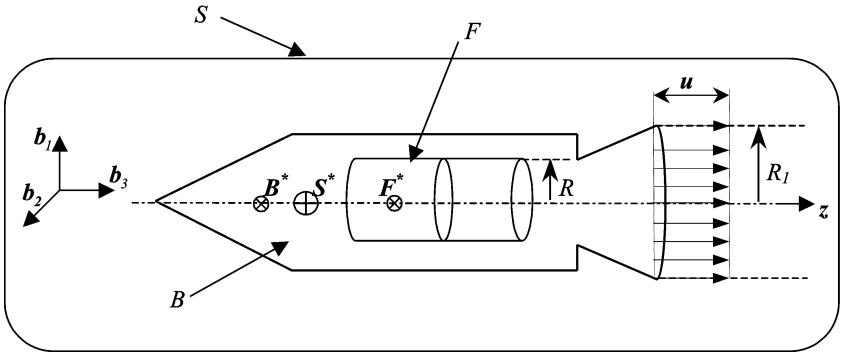

Figure 2.1. Two-body axisymmetric model.

constant mass section. Mass loss comes from the burning and expulsion of particles of the propellant. The model can provide for the existence of a nozzle; there is some flexibility in the geometric location of the fuel within the system; and various propellant depletion geometries can be explored with this model. The goal of this study is to use this two body axisymmetric model to examine how the attitude motion of a rocket system is influenced by substantial mass loss and by changes in various system parameters, and to compare the outcome with results obtained in previous studies that used much simpler models. In particular, we wish to explore the effect of the nozzle on attitude motion — a study that has not as yet been done, and that could not really be done with a less sophisticated model than the one employed here.

2 Equations of Attitude Motion

As stated earlier, the model used for this study is the two-body axisymmetric system as shown in Figure 2.1. B represents the entire system with the exception of the propellant, and it is assumed to constitute a constant mass, axisymmetric rigid body. For the purposes of this study, the fuel F is also assumed to be a rigid body, whose shape at ignition is that of a uniform, right, circular cylinder, with its axis aligned with that of the main body B. F is shown in a partially burned state in the figure; it is assumed to burn in such a way that its unburned part is always axisymmetric with respect to the longitudinal axis z of the original, unburned, cylindrical fuel. The overall system, that is, the combination of B and F is designated S and has its mass center at S^*. B^* and F^* are the mass centers of B and F respectively.

One version of the vector equation of attitude motion for the type of variable mass system under study here is given as equation (1) below. This equation comes from Eke and Wang [3], and is, in its simplified form, equivalent to versions of rotational equations derived by other authors [2, 7, 12]

$$\begin{aligned}\mathbf{M} = \mathbf{I}\cdot\alpha + \omega\times\mathbf{I}\cdot\omega + \left(\frac{d\mathbf{I}}{dt}\right)\cdot\omega + \int_C \rho[\mathbf{p}\times(\omega\times\mathbf{p})](\mathbf{v}\cdot\mathbf{n})\,dS \\ + \int_C \rho\omega\times(\mathbf{p}\times\mathbf{v})\,dV + \frac{d}{dt}\int_C \rho(\mathbf{p}\times\mathbf{v})\,dV + \int_C \rho(\mathbf{p}\times\mathbf{v})(\mathbf{v}\cdot\mathbf{n})\,dS.\end{aligned} \tag{1}$$

In this equation, $\mathbf{M}$ is the sum of the moments of external forces on the system S about the system mass center, S^*; $\mathbf{I}$ is the system's instantaneous central inertia dyadic; $\mathbf{p}$ is the position vector from S^* to a generic particle of the system; ρ is the mass density; $\mathbf{v}$ is the velocity of a generic particle relative to B; C is a fictitious outer shell that encloses the whole system; $\mathbf{n}$ is a unit vector that is normal to, and pointing outwards of the surface C; and ω and α are, respectively, the inertial angular velocity and angular acceleration of the main body B of the system. All the vector and dyadic time derivatives are taken in the reference frame of the rigid body B.

There are at least two arguments that can be used to bring equation (1) down to a manageable form. First, one can exploit the symmetry of the system and assume that at steady state, the motion of gas particles inside the system's combustion chamber is symmetric relative to the z-axis, and that whirling motion (helical motion) of these particles relative to B is negligible. Because of these assumptions, the last three terms on the right hand side of equation (1) vanish (see details in [3]), and the equation reduces to

$$\mathbf{M} = \mathbf{I} \cdot \alpha + \omega \times \mathbf{I} \cdot \omega + \left(\frac{d\mathbf{I}}{dt} \cdot \omega \right) + \int_C \rho \left[\mathbf{p} \times (\omega \times \mathbf{p}) \right] (\mathbf{v} \cdot \mathbf{n}) \, dS. \tag{2}$$

A second argument that can be used to obtain the same result is based on the fact that there are situations where the velocity $\mathbf{v}$ of the gas particles can be considered negligible within the system's boundary but not at an exit from the boundary, such as the nozzle. An example is an inflated balloon with a small hole. Velocities of gas particles within the balloon are negligible in magnitude compared to those of gas particles leaving through the hole. Whenever $\mathbf{v}$ can be considered negligible within a system's boundary, but is finite and forms a symmetric field at each exit from the system, equation (1) reduces once more to equation (2). It is reasonable to assume that such is approximately the situation for the system under study.

Equation (2) can be broken down into three scalar components by expressing each of the terms on the right hand side of the equation in terms of the unit vectors $\mathbf{b}_i$ $(i = 1, 2, 3)$ shown in Figure 2.1. Assuming that the velocity distribution of the gas particles as they leave the nozzle exit plane is uniform as shown in Figure 2.1, we have that

$$\mathbf{v} \cdot \mathbf{n} = u = \text{const} \tag{3}$$

over the nozzle exit. If we then restrict the study to the case of zero external moment $(\mathbf{M} = \mathbf{0})$, equation (2) takes the scalar forms

$$I\dot{\omega}_1 + \left[\dot{I} - \dot{m} \left(z_e^2 + \frac{R_1^2}{4} \right) \right] \omega_1 + \left[(J - I)\omega_3 \right] \omega_2 = 0, \tag{4}$$

$$I\dot{\omega}_2 + \left[\dot{I} - \dot{m} \left(z_e^2 + \frac{R_1^2}{4} \right) \right] \omega_2 - \left[(J - I)\omega_3 \right] \omega_1 = 0, \tag{5}$$

$$J\dot{\omega}_3 + \left(\dot{J} - \frac{\dot{m} R_1^2}{2} \right) \omega_3 = 0, \tag{6}$$

where m represents the instantaneous mass of the system, I and J are, respectively, the central transverse and spin moment of inertia for the system, z_e is the distance from S^* to the nozzle exit plane, R_1 is the radius of the circular nozzle exit area, and ω_i $(i = 1, 2, 3)$ are the scalar components of the inertial angular velocity of B in the $\mathbf{b}_i$ $(i = 1, 2, 3)$ unit

vector basis. We note here that the unit vectors $\mathbf{b}_i$ are assumed fixed to the body B. Details of the transition from equation (2) to (4), (5), and (6) can be found in several places, including Morris [10].

Equations (4) through (6) can be non-dimensionalized as follows. First, we note that the rate, m_r, of mass depletion from the system can be written as a surface integral

$$M_r = -\dot{m} = \int (\mathbf{v} \cdot \mathbf{n}) \rho \, dS = \pi \rho u R_1^2 = \text{const}, \tag{7}$$

where ρ is the mass density of the fluid products of combustion — considered constant over the nozzle exit plane. The time, t_b, taken for the mass m_F of the propellant to go from its initial value, m_{F0}, to the final value of zero (that is, burnout) can be expressed as

$$t_b = m_{F0}/m_r. \tag{8}$$

We choose as dimensionless time variable, the quantity τ given by

$$\tau = t/t_b = (m_r/m_{F0})t, \tag{9}$$

where t is time measured from the beginning of the propellant burn (ignition). We then note that $\tau = 0$ at propellant ignition, and $\tau = 1$ at burnout. Furthermore,

$$\frac{d\tau}{dt} = \frac{1}{t_b}, \tag{10}$$

so that the time derivative of any quantity can be written as

$$\dot{(\,\cdot\,)} = \frac{d(\,\cdot\,)}{dt} = \frac{d(\,\cdot\,)}{d\tau} \cdot \frac{d\tau}{dt} = \frac{1}{t_b} \cdot \frac{d(\,\cdot\,)}{d\tau} = \frac{1}{t_b}(\,\cdot\,)', \tag{11}$$

where a prime $(\,')$ indicates derivative with respect to τ. We define other dimensionless quantities as

$$\overline{m} = m/m_{F0}, \quad \bar{I} = I/m_{F0}R^2, \quad \bar{J} = J/m_{F0}R^2, \quad \text{and} \quad \overline{\omega}_i = \omega_i t_b \quad (i = 1, 2, 3) \tag{12}$$

and use these to convert equations (4)–(6) to

$$\bar{I}\overline{\omega}_1' + \left\{ \bar{I}' - \overline{m}' \left[\left(\frac{z_e}{R} \right)^2 + \frac{\beta^2}{4} \right] \right\} \overline{\omega}_1 + [(\bar{J} - \bar{I})\overline{\omega}_3]\overline{\omega}_2 = 0, \tag{13}$$

$$\bar{I}\overline{\omega}_2' + \left\{ \bar{I}' - \overline{m}' \left[\left(\frac{z_e}{R} \right)^2 + \frac{\beta^2}{4} \right] \right\} \overline{\omega}_2 + [(\bar{J} - \bar{I})\overline{\omega}_3]\overline{\omega}_1 = 0, \tag{14}$$

and

$$\bar{J}\overline{\omega}_3' + \left(\bar{J}' - \overline{m}' \frac{\beta^2}{2} \right) \overline{\omega}_3 = 0. \tag{15}$$

In these equations, R is the external radius of the cylindrical propellant, and β is the ratio R_1/R.

From equation (15),

$$\frac{\overline{\omega}_3(\tau)}{\overline{\omega}_3(0)} = \exp\left[-\int_0^\tau \frac{\psi(\tau)}{\bar{J}} \, d\tau \right], \tag{16}$$

where

$$\psi(\tau) = \bar{J}' - \overline{m}' \frac{\beta^2}{2}. \tag{17}$$

By defining a dimensionless, complex angular velocity

$$\overline{\omega}_T = \overline{\omega}_1 + i\overline{\omega}_2, \tag{18}$$

where $i = \sqrt{-1}$, equations (13) and (14) are combined to give

$$\frac{\overline{\omega}_T(\tau)}{\overline{\omega}_T(0)} = \left\{ \exp\left[-\int_0^\tau \frac{\varphi(\tau)}{\bar{I}}\, d\tau \right] \right\} \cdot \left[\exp\left(i \int_o^\tau \Theta\, d\tau \right) \right], \tag{19}$$

where

$$\varphi(\tau) = \bar{I}' - \overline{m}' \left[\left(\frac{z_e}{R} \right)^2 + \frac{\beta^2}{4} \right] \tag{20}$$

and

$$\Theta = [(\bar{J}/\bar{I}) - 1]\, \overline{\omega}_3. \tag{21}$$

The function $\varphi(\tau)$ determines the magnitude of the transverse angular velocity vector, $\Theta(\tau)$ governs the frequency, and $\psi(\tau)$ [see equation (17)] tells us whether the spin rate will increase or decrease with τ. We will limit this study to an examination of how the spin rate and transverse angular velocity magnitude vary with propellant burn.

3 Spin Motion

We now take an in depth look at the spin rate, to see how it is affected by mass loss or propellant burn. It is clear from equations (16) and (17) that expressions for the system's mass and inertia as functions of the dimensionless time variable τ are needed in order to make progress with the study of the spin rate. On the other hand, these functions can only be determined if a propellant depletion geometry is stipulated. For this study, we choose to examine the case of a burn that is an idealization of a common burn pattern in solid rocket motors. In this burn, which is often referred to as radial burn, it is imagined that the propellant has the shape of a hollow cylinder at ignition. The interior surface is ignited, and the fuel then burns radially outwards in a uniform manner, so that the interior surface always remains cylindrical. Figure 3.1 shows an intermediate shape for the propellant during such a burn. We now proceed to determine the elements that are needed to express the function ψ in equation (17) in terms of the variable τ.

From Figure 3.1, the mass of the fuel just before ignition is

$$m_{F0} = \rho_F \pi L (R^2 - r_0^2) \tag{22}$$

and the mass m_F at a general instant during the burn is

$$m_F = \rho_F \pi L (R^2 - r^2). \tag{23}$$

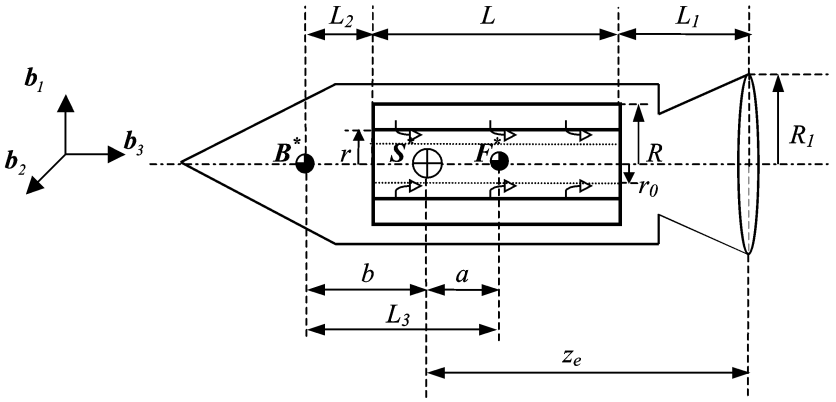

Figure 3.1. Rocket with radially burning propellant.

Here, L is the length of the cylindrical fuel, ρ_F is the mass density of F, r_0 is the initial internal radius of F, and r is the internal radius at some general instant after ignition. From equations (8), (22), and (23),

$$t_b = \frac{m_{F0}}{m_r} = \frac{m_{F0}}{-\dot{m}_F} = \frac{R^2 - r_0^2}{\dfrac{d}{dt}(r^2)}. \tag{24}$$

Equation (24) is integrated to give

$$r^2(t) = r_0^2 + \frac{R^2 - r_0^2}{t_b}\, t \tag{25}$$

so that

$$\left(\frac{r}{R}\right)^2 = \left(\frac{r_0}{R}\right)^2 = \left[1 - \left(\frac{r_0}{R}\right)^2\right]\tau = \gamma^2 + (1-\gamma^2)\tau, \tag{26}$$

where γ is the ratio r_0/R. We thus have from equations (22), (23), and (26), that the non-dimensional mass $\overline{m}_F$ for the propellant is

$$\overline{m}_F = \frac{m_F}{m_{F0}} = \frac{\rho_F \pi L(R^2 - r^2)}{\rho_F \pi L(R^2 - r_0^2)} = \frac{1 - (r/R)^2}{1 - (r_0/R)^2} = 1 - \tau, \tag{27}$$

which yields

$$\overline{m}' = \overline{m}'_F = -1. \tag{28}$$

In a similar way, we use equations (26) and (27) to show that the dimensionless axial inertia of the propellant F is given by

$$\bar{J}_F = \frac{J_F}{m_{F0}R^2} = \frac{\overline{m}_F}{2}\left[1 + \left(\frac{r}{R}\right)^2\right] = \left[\frac{1-\tau}{2}\right][1 + \gamma^2 + (1-\gamma^2)\tau]. \tag{29}$$

The overall system axial moment of inertia is thus given, in dimensionless form, as

$$\bar{J} = \bar{J}_B + \bar{J}_F = \bar{J}_B + \frac{1+\gamma^2}{2} - \gamma^2\tau - \frac{1-\gamma^2}{2}\tau^2. \tag{30}$$

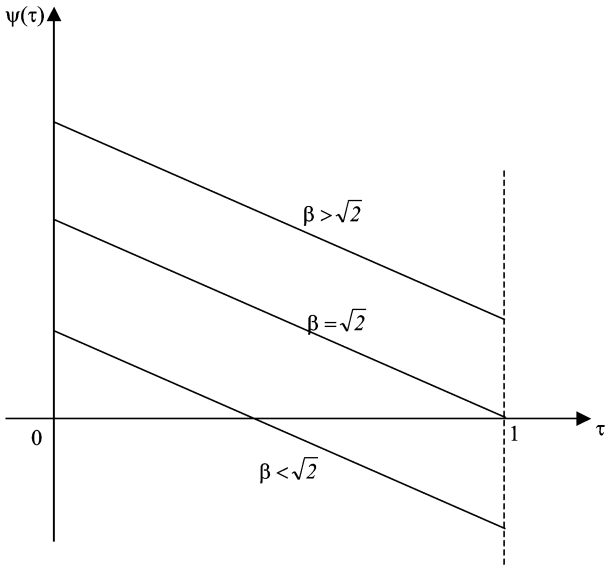

Figure 3.2. Possible shapes for $\psi(\tau)$.

Equations (28), (30), and (17) lead to

$$\psi(\tau) = \left[\frac{\beta^2}{2} - \gamma^2\right] + (\gamma^2 - 1)\tau. \tag{31}$$

3.1 Qualitative discussion

The function $\psi(\tau)$ is linear in τ with slope (γ^2-1), which is negative for the burn we have selected. Hence $\psi(\tau)$ decays linearly with τ, and $\psi(0) = \beta^2/2-\gamma^2$, with $\psi(1) = \beta^2/2-1$. $\psi(0)$ is almost certain to be positive for real rocket systems, since, for these systems one would expect $\gamma \ll 1$ and $\beta \geq 1$. For example, picking such conservative numbers as $\gamma = 0.5$, and $\beta = 1$ still results in $\psi(0) > 0$. On the other hand, $\psi(1)$ can, conceivably, take on a value that is either positive or negative depending on whether or not the quantity β, which we shall refer to in the remainder of this paper as the nozzle expansion ratio, is greater than or less than $\sqrt{2}$. Figure 3.2 summarizes the behavior of the function $\psi(\tau)$ for three values of β. We conclude from this figure that the spin rate will always decrease initially. This trend will continue all the way to burnout if the nozzle expansion ratio is greater than some threshold value, β_L ($\sqrt{2}$ for radial burn). If β happens to be less than β_L, then, the decreasing trend in the spin rate will be reversed at some point during the burn, and the spin rate will increase for the remainder of the burn. The point at which this change in trend occurs is $(\psi = 0)$

$$\tau = (\beta^2/2 - \gamma^2)/(1 - \gamma^2). \tag{32}$$

For a variable mass cylinder with no nozzle, $\beta = 1$, and only one scenario $(\beta < \beta_L)$ is possible. As explained above for this case, the spin rate will decrease initially until τ attains a value given by equation (32). After this, the spin rate increases till burnout.

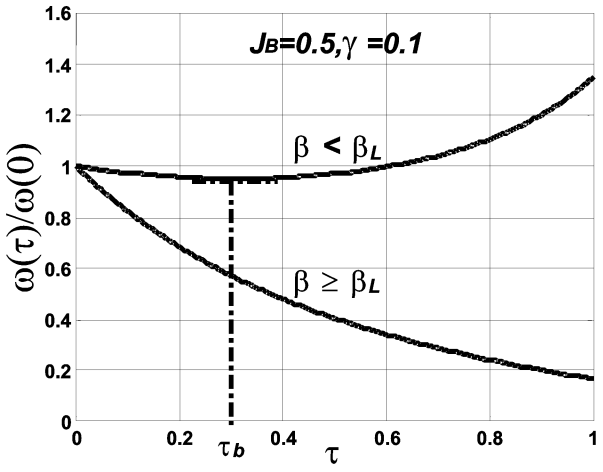

Figure 3.3. Spin rate for radial burn.

By substituting $\beta = 1$ into equation (32), and putting the resulting value for τ into equation (26), we find that the minimum value of the spin rate will occur when the ratio $r/R = 1/\sqrt{2}$. This is the same result obtained in [6] for the simple variable mass cylinder.

3.2 Closed form solution

If equations (30) and (31) are substituted into equation (16), a closed form solution can be obtained for equation (16) as follows:

$$\frac{\overline{\omega}_3(\tau)}{\overline{\omega}_3(0)} = \left[\frac{\Pi^2 - \gamma^4}{\Pi^2 - [\gamma^2 + (1-\gamma^2)\tau]^2}\right] \times \exp\left\{\frac{-\beta^2}{\Pi}\left[\tanh^{-1}\frac{[\gamma^2 + (1-\gamma^2)\tau]}{\Pi} - \tanh^{-1}\frac{\gamma^2}{\Pi}\right]\right\}, \tag{33}$$

where

$$\Pi = \sqrt{2\bar{J}_B(1-\gamma^2+1)}. \tag{34}$$

The curves shown in Figure 3.3 come from equation (33), and they confirm the initial negative slope of the spin rate, and the fact that the spin rate can change from a decreasing to an increasing function of τ during a propellant burn, for small values of the nozzle expansion ratio. It would appear, from equation (33) that besides the parameters γ and β, the axial inertia $\bar{J}_B$ can also play a role in the behavior of the spin rate. Figure 3.4 is obtained from equation (33), and shows how a change in axial inertia $\bar{J}_B$ for the main body B affects the spin rate. The smaller the value of $\bar{J}_B$ the more the spin rate curve deviates from that which is expected from a constant mass rigid body; that is, a constant. This is certainly in agreement with engineering intuition. However, the basic character of the spin rate curve is not affected by a change in $\bar{J}_B$. It turns out that a change in the ratio γ of the initial internal radius to external radius of the fuel without a change in $\bar{J}_B$ has minimal effect on the spin rate.

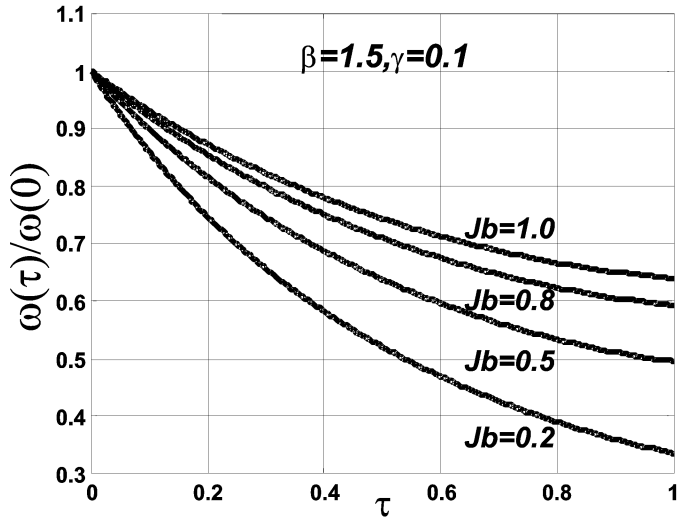

Figure 3.4. Influence of spin interia on the spin rate.

3.3 Stable spin

It is not desirable to have the spin rate grow substantially, nor is it acceptable for the spin rate to decrease excessively during a propellant burn. In one case, the system's structural integrity can become impaired, and in the other case, there is loss of spin rigidity. It is therefore useful to find ways to limit variations in spin rate during a burn. One way to accomplish this is to force the spin rate at the end of the burn to be the same as that at ignition; that is, $\overline{\omega}_3(1) = \overline{\omega}_3(0)$. From equation (33), we have

$$\frac{\overline{\omega}_3(1)}{\overline{\omega}_3(0)} = \left[\frac{\Pi^2 - \gamma^4}{\Pi^2 - 1}\right] \cdot \exp\left\{\frac{-\beta^2}{\Pi}\left[\tanh^{-1}\frac{1}{\Pi} - \tanh^{-1}\frac{\gamma^2}{\Pi}\right]\right\} = 1, \tag{35}$$

which leads eventually to

$$\beta_b = \sqrt{\frac{\Pi \cdot \ln[(\Pi^2 - \gamma^4)/(\Pi^2 - 1)]}{\tanh^{-1}(1/\Pi) - \tanh^{-1}(\gamma^2/\Pi)}}. \tag{36}$$

Equation (36) gives the value of the nozzle expansion ratio that will bring the spin rate at burnout back to its value at ignition, and in so doing, limit the overall variation in the spin rate. Figure 3.5 shows that the necessary nozzle expansion ratio is sensitive to the axial inertia $\bar{J}_B$ of the main rocket body, especially at low values of $\bar{J}_B$. Figure 3.6 gives an indication of the level of sensitivity of the spin rate to deviations in the choice of β. This figure also shows that when β is taken to be β_b, the difference between the extreme values of the spin rate is not as large as when $\beta \neq \beta_b$.

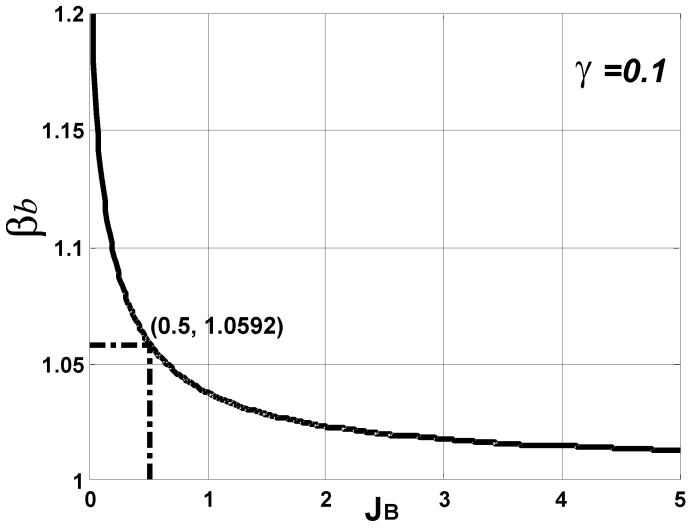

Figure 3.5. Relationship between $\bar{J}_B$ and β_b.

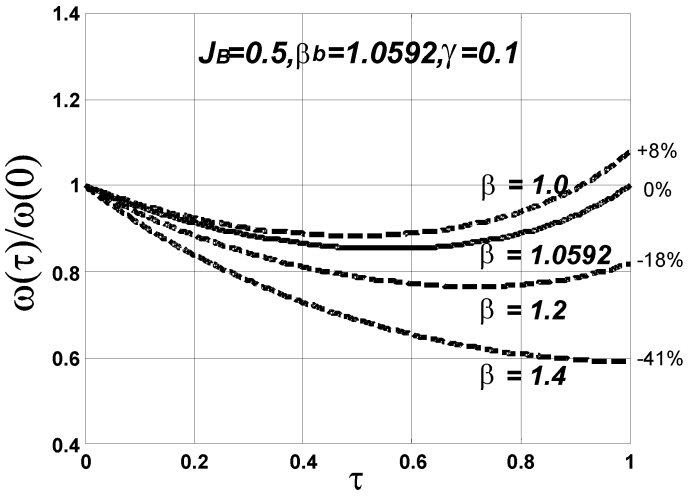

Figure 3.6. Spin rate deviations for $\beta \neq \beta_b$.

4 Transverse Angular Speed

The system's central transverse moment of inertia can be written, in non-dimensional form as

$$\bar{I} = \bar{I}_B + \bar{I}_F + (m_B b^2 = m_F a^2)/m_{F0}R^2, \tag{37}$$

where the subscripts B and F refer to the main body and the fuel respectively, and the distances a and b as well as other distances such as L, L_i $(i = 1, 2, 3)$ are as shown in Figure 3.1. The transverse inertia of B is $\bar{I}_B = I_B/m_{F0}R^2$. Keeping in mind that we are assuming a radial burn for the fuel,

$$\bar{I}_F = \frac{I_F}{m_{F0}R^2} = \overline{m}_F\left[\frac{1}{4}+\frac{1}{4}\left(\frac{r}{R}\right)^2+\frac{1}{12}\left(\frac{L}{R}\right)^2\right] = (1-\tau)\left[\frac{1+\gamma^2+(1-\gamma^2)\tau}{4}+\frac{\delta^2}{12}\right]. \tag{38}$$

The distances a and b can be expressed as

$$a = \frac{m_B L_3}{m_B + m_F} \tag{39}$$

and

$$b = \frac{m_F L_3}{m_B + m_F}. \tag{40}$$

Substituting equations (38), (39), and (40) into (37), we obtain, after some algebra,

$$\bar{I} = \bar{I}_B + (1-\tau)\left[\frac{1+\gamma^2+(1-\gamma^2)\tau}{4} + \frac{\delta^2}{12}\right] + \frac{\overline{m}_B(1-\tau)\delta_3^2}{\overline{m}_B + 1 - \tau} \tag{41}$$

so that

$$\bar{I}' = -\left\{\frac{\gamma^2+(1-\gamma^2)\tau}{2} + \frac{\delta^2}{12} + \left(\frac{\overline{m}_B\delta_3}{\overline{m}_B + 1 - \tau}\right)^2\right\}. \tag{42}$$

The distance

$$z_e = L_1 + \frac{L}{2} + a. \tag{43}$$

Hence, equations (43), (39), and (27) give

$$\frac{z_e}{R} = \frac{(\overline{m}_B + \overline{m}_F)(\delta_1 + \delta/2) + \overline{m}_B\delta_3}{\overline{m}_B + \overline{m}_F} = \frac{(\overline{m}_B + 1 - \tau)(\delta_1 + \delta/2) + \overline{m}_B\delta_3}{\overline{m}_B + 1 - \tau}, \tag{44}$$

where $\delta = L/R$, and $\delta_i = L_i/R$ $(i = 1, 2, 3)$. From equations (20), (28), (42), and (44),

$$\varphi(\tau) = -\left[\frac{\gamma^2+(1-\gamma^2)\tau}{2}\right] + \frac{\delta^2}{6} + \delta\delta_1 + \delta_1^2 + \frac{\beta^2}{4} + \frac{2\overline{m}_B\delta_3}{\overline{m}_B + 1 - \tau}\left(\frac{\delta}{2} + \delta_1\right). \tag{45}$$

4.1 Qualitative discussion of transverse motion

The transverse angular speed is given by [see equation (19)]

$$\left|\frac{\overline{\omega}_T(\tau)}{\overline{\omega}_T(0)}\right| = \exp\left[-\int_0^\tau \frac{\varphi(\tau)}{\bar{I}}\, d\tau\right]. \tag{46}$$

The function $\bar{I}$ decreases with τ but is always positive. Hence, the sign of $\varphi(\tau)$ determines whether the transverse rate increases or decreases with the burn. We can rewrite equation (45) as

$$\varphi(\tau) = \varphi_1(\tau) + \varphi_2(\tau) \tag{47}$$

where

$$\varphi_1(\tau) = -\left[\frac{\gamma^2 + (1-\gamma^2)\tau}{2}\right] \tag{48}$$

and

$$\varphi_2(\tau) = \frac{\delta^2}{6} + \delta\delta_1 + \delta_1^2 + \frac{\beta^2}{4} + \frac{2\overline{m}_B\delta_3}{\overline{m}_B + 1 - \tau}\left(\frac{\delta}{2} + \delta_1\right). \tag{49}$$

The function φ_1 is clearly negative, since $\gamma < 1$. On the other hand, φ_2 is positive because δ, δ_1, δ_3, β and $\overline{m}_B$ are all positive quantities for real rocket systems, and $0 \le \tau \le 1$. At $\tau = 0$, $\varphi_1 = -\gamma^2/2$; and, since $\gamma = r_0/R$ would be expected to be less than $1/2$ for a real system, $|\varphi_1| \le 1/8$. Similarly, $\varphi_2 > \beta^2/4 > 1/4$ in practice. Hence, $\varphi(0)$ is likely to be positive. As τ varies between 0 and 1, φ_1 decreases linearly with τ while φ_2 increases with τ. It appears unlikely that φ_2 will ever become less than φ_1 in absolute value, or that φ will change sign from positive to negative during the propellant burn. Thus, the transverse angular speed is likely to decrease between ignition and burnout.

There are several factors that can change this state of affair for the transverse angular speed. They include small values of what may be referred to as the propellant aspect ratio $\delta = L/R$, low values of the nozzle expansion ratio β, proximity of the propellant grain to the nozzle (δ_1), and closeness of the propellant center of mass to that of the rocket's main body. These can lower the value of φ_2 to the point where $|\varphi_2| < |\varphi_1|$ and $\varphi < 0$. Of these, the parameters that a rocket designer has most control over are δ and β.

We note here that relatively recent studies [4, 6] that used the cylinder model came to the conclusion that a "fat and short" propellant grain (i.e. low δ) can cause the transverse angular speed to grow without bounds for a radial burn. This paper arrives at the same result, but adds another component that the nozzle expansion ratio can also have an important damping influence on the transverse angular speed. In fact, a large enough expansion ratio can, single-handedly, reverse the potential for a runaway growth in transverse rate. For instance, the maximum value that φ_1 can have during a radial burn is [see equation (48)] $-1/2$, and this occurs at $\tau = 1$. Hence, it suffices that $\beta \ge \sqrt{2}$ [see equation (49)] to guarantee that $\varphi > 0$ and that $\overline{\omega}_T$ will decrease with the burn.

Figure 4.1 is obtained by numerical integration of equation (46), and shows the transverse angular speed as a function of the time variable τ. This figure confirms that a low value of δ, coupled with a small β can indeed cause the transverse rate to reverse its initial decreasing trend sometime during the burn, and increase continuously through burnout.

5 Modified Radial Burn

So far, what has been presented is a general study of the radial burn. We now move briefly to the case where the system mass center, S^*, does not shift relative to the rocket's main body B. In other words, we assume that, prior to ignition, the mass centers B^* of the rocket body and F^* of the solid fuel are coincident, so that S^* is also located at

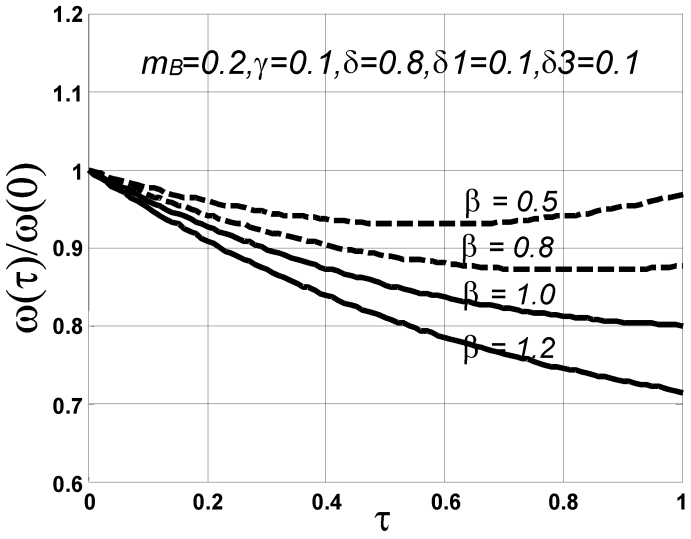

Figure 4.1. Transverse angular speed.

the same point. During a radial burn, F^* does not shift relative to B. Hence, all three points F^*, B^* and S^* remain coincident throughout the burn. This can be accomplished in a real system by balancing the system in such a way that S^* and F^* (or F^* and B^*) coincide prior to propellant ignition. Our interest here is to see whether there is anything to be gained, from the point of view of attitude dynamics, in balancing the system in this way.

As before, the focus here is again on the functions $\varphi(\tau)$ and $\psi(\tau)$ given in equations (45) and (31) respectively. In this case, the parameter δ_3 becomes zero. The function φ_1 is unaffected, but the last term of φ_2 (a positive term) drops. Thus, $\varphi(0)$ is reduced somewhat but remains positive. It is now slightly easier for $\varphi(1)$ to become negative, leading to a possibility of transverse rate increase during a propellant burn. The expression for $\psi(\tau)$ remains as given in equation (31), so the spin rate is unaffected by the proposed change. Overall, we can state that there is no advantage whatsoever in balancing the system in such a way as to avoid system mass center shift. In fact, such an action renders the system more sensitive to divergence in transverse angular speed.

6 Conclusion

This study deals with the dynamic behavior of spinning bodies of the rocket type, that lose mass while moving in a torque-free environment. The attitude behavior of systems of this type is known to be influenced by the manner in which mass loss affects the geometry of the system. One specific mass loss scenario — the radial burn — was studied. This scenario assumes that the propellant of the rocket system is a hollow cylindrical solid whose internal radius grows uniformly as the propellant burns. This appears to restrict the study to rockets with solid propellants. However, the results of this study can in fact be applied to some systems with liquid propellant. When liquid propellant

is used in rocket systems that spin, it is generally distributed in several tanks positioned symmetrically with respect to the spin axis. As the solid portion of the system spins, centrifugal effects cause the liquid propellant to move outward and the overall behavior of the fuel system becomes very similar to that of a solid propellant undergoing radial burn.

Results obtained indicate that the spin rate always begins by decreasing with propellant burn. If the ratio, β, of the nozzle exit radius to the external radius of the propellant grain is greater than $\sqrt{2}$, then the spin rate will continue to decrease until propellant burnout. If, however, the value of β is less than $\sqrt{2}$, the spin rate attains a minimum value during the burn, begins to increase as the burn proceeds, and continues this trend through burnout. The value of the nozzle expansion ratio thus plays a pivotal role in determining the character of the spin rate curve.

The transverse angular speed will normally decrease with propellant burn. However, there are circumstances under which growth in transverse angular speed becomes possible. Such a situation can arise if the ratio of the length of the propellant grain to its radius is very small at the same time that the nozzle expansion ratio is also small. In this case, the curve of the transverse rate as a function of propellant burn decreases initially, but flattens out sometime during the burn, and then rises for the remainder of the burn. This study brings out the important role that the nozzle expansion ratio can play in determining how both the spin rate and the transverse angular speed evolve with propellant burn.

Balancing a rocket system so that its mass center does not shift during propellant burn actually renders the system more prone to growth in transverse rate if the nozzle expansion ratio is low. Another way of viewing this is that studies that assume no shift in system mass center will in general produce conservative results.

References

[1] Buquoy, G. *Exposition d'un Nouveau Principe General de Dynamique*. Paris, 1816.

[2] Eke, F.O. and Mao, T.C. On the dynamics of variable mass systems. *The Int. J. of Mech. Engin. Education* **30**(2) (2002) 123–137.

[3] Eke, F.O. and Wang, S.M. Equations of motion of two-phase variable mass systems with solid base. *ASME J. of Appl. Mech.* **61** (1994) 855–860.

[4] Eke, F.O. and Wang, S.M. Attitude behavior of a variable mass cylinder. *ASME J. of Appl. Mech.* **62**(4) (1995) 935–940.

[5] Kovalev, A.M. Stability of stationary motions of mechanical systems with rigid body as basic element, *Nonlinear Dynamics and Systems Theory* **1**(1) (2001) 81–96.

[6] Mao, T.C. and Eke, F.O. Attitude dynamics of a torque-free variable mass cylindrical body. *J. Astronautical Sci.* **48**(4) (2000) 435–448.

[7] Meirovitch, L. General motion of a variable mass flexible rocket with internal flow. *J. Spacecraft and Rockets* **7**(2) (1970) 186–195.

[8] Meshcherskii, I.V. *Dynamics of a Point of Variable Mass*. St. Petersburg, 1897 (reprinted in: I.V. Meshcherskii, *Works on the Mechanics of Variable-Mass Bodies*. 2nd Edition, Moscow, 1952).

[9] Meshcherskii, I.V. Equations of motion of a variable-mass point in the general case. *St. Petersburg Polytechnic University News* **1** (1904) 77–118.

[10] Morris, M.J. *Effect of Mass Variation on the Attitude Motion of Rocket Systems*. M.S. Thesis, University of California, Davis, CA, 2001.

[11] Thomson, W.T. *Introduction to Space Dynamics*. John Wiley & Sons, Inc., New York, 1961.

[12] Thomson, W.T. Equations of motion for the variable mass system. *AIAA J.* **4**(4) (1966) 766–768.
[13] Thomson, W.T. and Reiter, G.S. Jet damping of a solid rocket: theory and flight results. *AIAA J* **3**(3) (1965) 413–417.
[14] Wang, S.M. and Eke, F.O. Rotational dynamics of axisymmetric variable mass systems. *ASME J. Appl. Mech.* **62** (1995) 970–974.